JVI Journals.ASM.org

The Open Chromatin Landscape of Kaposi's Sarcoma-Associated Herpesvirus

Isaac B. Hilton,[a,b] Jeremy M. Simon,[a,c] Jason D. Lieb,[i] Ian J. Davis,[a,d,e,f] Blossom Damania,[a,g,h] Dirk P. Dittmer[a,g,h]

Lineberger Comprehensive Cancer Center,[a] Curriculum in Genetics and Molecular Biology,[b] Curriculum in Bioinformatics and Computational Biology,[c] Department of Genetics,[d] Carolina Center for Genome Sciences,[e] Department of Pediatrics,[f] Program in Global Oncology,[g] and Department of Microbiology and Immunology,[h] University of North Carolina at Chapel Hill, Chapel Hill, North Carolina, USA; Lewis-Sigler Institute of Integrative Genomics, Princeton University, Princeton, New Jersey, USA[i]

Kaposi's sarcoma-associated herpesvirus (KSHV) is an oncogenic gammaherpesvirus which establishes latent infection in endothelial and B cells, as well as in primary effusion lymphoma (PEL). During latency, the viral genome exists as a circular DNA minichromosome (episome) and is packaged into chromatin analogous to human chromosomes. Only a small subset of promoters, those which drive latent RNAs, are active in latent episomes. In general, nucleosome depletion ("open chromatin") is a hallmark of eukaryotic regulatory elements such as promoters and transcriptional enhancers or insulators. We applied formaldehyde-assisted isolation of regulatory elements (FAIRE) followed by next-generation sequencing to identify regulatory elements in the KSHV genome and integrated these data with previously identified locations of histone modifications, RNA polymerase II occupancy, and CTCF binding sites. We found that (i) regions of open chromatin were not restricted to the transcriptionally defined latent loci; (ii) open chromatin was adjacent to regions harboring activating histone modifications, even at transcriptionally inactive loci; and (iii) CTCF binding sites fell within regions of open chromatin with few exceptions, including the constitutive LANA promoter and the vIL6 promoter. FAIRE-identified nucleosome depletion was similar among B and endothelial cell lineages, suggesting a common viral genome architecture in all forms of latency.

Kaposi's sarcoma-associated herpesvirus (KSHV), or human herpesvirus 8, is the most recently discovered human herpesvirus and is a member of the gammaherpesvirus subfamily (1). It is linked with three human malignancies of either endothelial or B cell origin: Kaposi's sarcoma (KS; of endothelial cell origin), primary effusion lymphoma (PEL; of B cell origin), and a variant of multicentric Castleman's disease (MCD; of B cell origin) (1–3).

All herpesviruses display two alternating forms of infection: latency and productive lytic infection. During KSHV latency, the ~140-kb viral genome exists as a nonintegrated circular nucleosome-associated episome (reviewed in references 4, 5, and 6). The KSHV genome includes over 80 predicted open reading frames (ORFs), 22 known viral microRNAs (miRNAs), and several long noncoding RNAs (7–9; also reviewed in references 10 and 11). During latent infection, only a few viral genes are transcribed, including those within the KSHV latency locus (12–14). This locus employs a complex transcriptional circuitry to generate key viral messages, including the mRNAs coding for the KSHV latency-associated nuclear antigen (LANA; ORF73) (12, 14–18), the viral cyclin homolog vCyclin (ORF72), vFLIP (ORF71), and Kaposin, as well as all 12 viral microRNA genes. Each miRNA gene encodes one pre-miRNA, which can give rise to two mature miRNAs, albeit at widely differing ratios. LANA is necessary and sufficient to tether the KSHV genome to the human chromosome, thereby ensuring coordinated genome duplication and segregation during host cell division (reviewed in reference 19).

Prior studies established histone occupancy on the latent KSHV episome (20–22), mapping specific activating and repressive histone signatures, as well as DNA methylation status, and occupancy of RNA polymerase II (PolII), LANA, and CTCF/cohesin (23–28). Most of these prior studies were conducted solely in the prototypical BCBL1 cell line. Many, but not all, achieved single-nucleotide resolution using chromatin immunoprecipitation-sequencing (ChIP-seq). In comparison to mapping individual histone modifications, little is known about chromatin organization, or about how regions of open chromatin in KSHV are integrated with the "histone code." Thanks to the authors of all prior studies making their raw data publicly available, here we were able to expand on their work and to add our detailed genome-wide map of KSHV nucleosome depletion in multiple KSHV-infected cell lines at single-nucleotide resolution.

The detection of nucleosome depletion has classically been accomplished by techniques such as DNase I hypersensitivity, which rely upon the differential in sensitivity to nuclease digestion of open chromatin relative to regions enriched in nucleosomes (29–31). An alternative method, called *f*ormaldehyde-*a*ssisted *i*solation of *r*egulatory *e*lements (FAIRE), also identifies regions of open chromatin but, however, without the use of enzymes (32–35) and has been employed in several different eukaryotes, cell lines, tissues, and pathogens (34, 36–43). FAIRE is based on differences in cross-linking efficiency between DNA bound to nucleosomes and DNA in nucleosome-depleted regions (32). Regions detected by FAIRE are concordant with DNase I hypersensitivity and anticorrelated with micrococcal nuclease (MNase) digestion. The efficacy of FAIRE is not dependent upon antibodies or enzymes, making it a more robust approach (35, 37, 39, 43). For

Received 27 June 2013 **Accepted** 19 August 2013
Published ahead of print 28 August 2013
Address correspondence to Dirk P. Dittmer, ddittmer@med.unc.edu.
Supplemental material for this article may be found at http://dx.doi.org/10.1128/JVI.01685-13.

doi:10.1128/JVI.01685-13

TABLE 1 Summary of sequencing data[a]

Sample	No. of raw reads	No. aligned with KSHV[b]	Fraction (%)	Mean coverage (fold)	No. of FAIRE peaks[c]
BC1	9,023,981	31,987	0.35	11.59	24
BCBL1	26,983,911	26,786	0.10	9.71	27
KSHV-BJAB	9,961,339	25,470	0.26	9.22	28
KSHV-HUVEC	72,447,917	17,288	0.02	6.26	23
L1-TIVE	79,435,320	5,653	0.01	2.05	15

[a] All raw reads have been submitted to the NIH archive under accession number XYZ.
[b] KSHV reference genome NC_009333.
[c] Using MACS2, assuming an average fragment size of 250 bp.

the purpose of these experiments, we refer to FAIRE peaks as nucleosome-depleted or open chromatin regions.

In this study, we found that histone modifications associated with transcriptional activity (H3K9-ac, H3K14-ac, and H3K4-me3) are enriched near sites of nucleosome depletion as identified by FAIRE. Additionally, CTCF binding sites coincided with many, but not all, nucleosome-depleted loci in the KSHV genome. In fact, we could for the first time discern two types of open chromatin loci on the KSHV episome: those associated with CTCF binding, which mapped to regions of immediate early and early genes, known to be transcriptionally silent during latency, and those free of CTCF, which mapped to transcriptionally active regions, such as the major latent promoter (LANA promoter [LANApc]) and the vIL6 promoter. Patterns of nucleosome depletion in KSHV were largely conserved across different latently infected cell types, among multiple KSHV isolates, and independently of the episomal copy number in a latently infected cell.

MATERIALS AND METHODS

Cell culture. Latent KSHV-infected lymphoma cell lines (BC1, BCBL1, and KSHV-BJAB) were cultured in RPMI medium supplemented with 10% fetal bovine serum (FBS) as previously described (44), with the exception that KSHV-BJAB cells were maintained under 0.2-mg/ml hygromycin selection (45). Latent KSHV-infected endothelial L1-TIVE cells (46) were grown in Dulbecco modified Eagle medium (DMEM) supplemented with 100 μg/ml streptomycin sulfate and 100 U/ml penicillin G and 5% FBS. Latently infected KSHV-human umbilical vein endothelial cells (HUVEC) were cultured in endothelial growth medium (EGM-2; Clonetics) supplemented with 0.5 μg/ml puromycin as previously described (47).

FAIRE-seq. Chromatin was isolated from ~1.0×10^7 cells and subjected to FAIRE as detailed previously (35). Briefly, cells were cross-linked with formaldehyde, lysed, and then sonicated to shear DNA to an average fragment length of 200 to 400 bp. Sheared DNA was then collected by phenol-chloroform extraction. Two biological replicates of cell lines (BC1, KSHV-BJAB, KSHV-HUVEC, and L1-TIVE) were harvested and processed on different days to account for variation. FAIRE-enriched DNA was then prepared for sequencing using the Illumina Truseq DNA Sample Preparation Kit V2 (Illumina) per the manufacturer's instructions or was prepared by the UNC High-Throughput Sequencing Facility (BCBL1 and non-cross-linked BCBL1 control). Indexed samples were sequenced using the Illumina HiSeq 2000 or GAIIx (for BCBL1 samples) (UNC High-Throughput Sequencing Facility) sequencer with 50-bp single-end reads.

Sequence analysis. Reads were filtered using TagDust (48), and individual sequencing runs were aligned to the reference KSHV genome NC_009333 using Bowtie (49). Reads were permitted to align to up to four locations in the genome, but the single best possible alignment was chosen. Regions with significantly enriched FAIRE signal were differentiated from background using MACS2 (50), assuming that the average fragment size was 250 bp. Results from biological replicates were merged, and resulting BAM and BED files were imported into CLC Bio (version 5.5.1) software for graphical display and further analysis. Previously published KSHV histone modification data (20) were analyzed, and regions with signal 3 standard deviations above a baseline of no signal (from data set S1) were considered significant enrichment and imported into CLC Bio. CTCF and KSHV LANA ChIP-seq data (23) were aligned with NC_009333 in CLC Bio using Gene Expression Omnibus (GEO) data sets GSM941710 and GSM941712, respectively. Further statistical analysis was conducted in R version 2.15.2.

Microarray data accession number. The data sets generated in association with this publication have been deposited in NCBI's Gene Expression Omnibus and are accessible through GEO Series accession number GSE50581.

RESULTS

Open chromatin map of the KSHV episome. To determine the regions of latent open chromatin in KSHV, we performed FAIRE-seq on representative, latently infected cell lines. Table 1 summarizes the sequencing data. Because each latently infected PEL cell contains 20 to 50 viral genomes (51), we achieved sufficiently deep coverage and thus are confident in the detailed position of each FAIRE peak. Because KSHV-HUVEC and L1-TIVE contain lower numbers of copies of the viral genome (52), a smaller percentage of reads from those samples aligned with KSHV. Nevertheless, even in these cases the mean coverage was comparable to the mean coverage used for FAIRE-based analyses of the human genome (37). Confirming earlier data, most of the viral episome was covered in nucleosomes and not enriched for open chromatin by FAIRE.

First, we performed FAIRE-seq on the KSHV-infected PEL cell line BCBL1 and aligned the resulting sequence reads to the KSHV reference genome (NC_009333). We used the NCBI designated reference genome as the basis for comparison, rather than individual viral strain genomes, to attain common map positions across multiple samples. We showed earlier that with the exception of the repetitive regions, few large indels exist among KSHV strains (53). Of the ~2.6×10^7 total reads, 0.10% mapped to the KSHV genome in BCBL1 cells (Table 1). We used MACS2 to derive statistically significant nucleosome depletion (FAIRE peaks) at single-nucleotide resolution. Figure 1A shows a linear representation of the KSHV genome, and Fig. 1B shows the FAIRE-seq coverage (raw read counts) in BCBL1. Sites of significant FAIRE peak enrichment were not detected in samples processed without cross-linking (Fig. 1C). Note the difference in scale, with the highest FAIRE signal at 289-fold coverage and the highest non-cross-linked signal at 18-fold coverage. In addition, comparison of the normalized per-nucleotide coverage from DNA isolated from

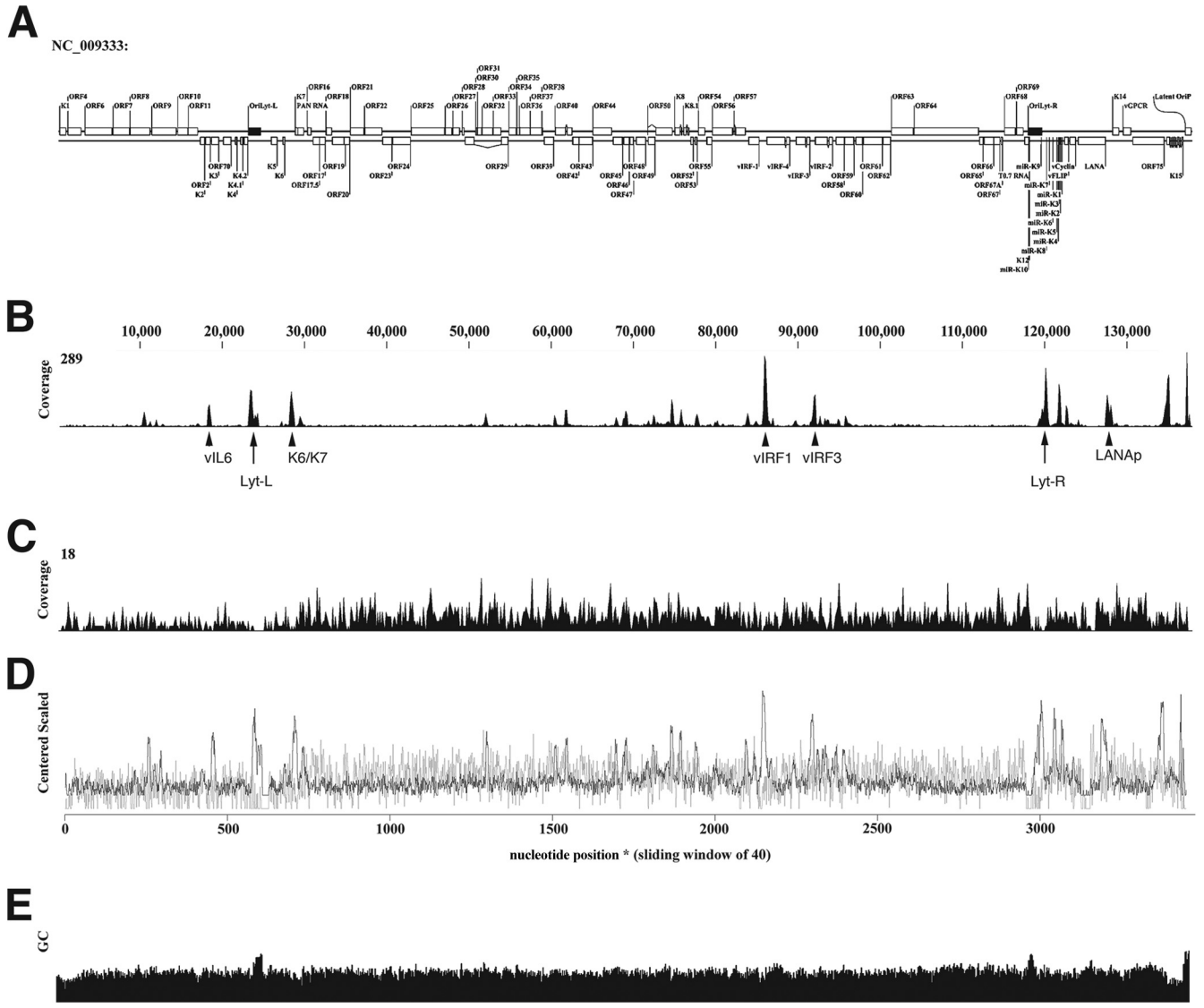

FIG 1 FAIRE-seq analysis of PEL (BCBL1). (A) Schematic of the KSHV genome (depicted linearly). Boxes indicate open reading frames (ORFs). ORFs on the upper strand are transcribed in rightward directions (with corresponding, predicted, or known regulatory regions on the left), and the lower strand corresponds to ORFs transcribed in the leftward direction (with corresponding, predicted, or known regulator regions on the right). (B) Read coverage data for FAIRE across the KSHV genome (BCBL1). Genome position is indicated on top. The maximal peak height was 289 reads covering a single nucleotide. (C) Read coverage of viral DNA from BCBL1 cells processed and sequenced as in panel B but not subjected to formaldehyde cross-linking. (D) Overlay of read coverage from formaldehyde cross-linked (black) and mock (gray)-treated BCBL1 cells. For comparison, raw count data were cube root transformed, median centered, and divided by their interquartile range/1.349. The normalized counts were then averaged using a 40-nucleotide sliding window. This procedure allows for a direct comparison of peak location, even though only approximately 1/10 of signal intensity was generated in the absence of cross-linking. (E) Predicted GC content across the KSHV reference genome NC_009333.

BCBL1 cells after formaldehyde cross-linking or mock treatment (Fig. 1D) demonstrated that the efficacy of the FAIRE-seq procedure was not biased by sample processing or high-throughput sequencing. The coverage obtained was unrelated to viral GC content (Fig. 1E). Except for the two lytic origins of replication and the terminal repeat (TR) latent replication origin, GC content was largely uniform across the genome.

As expected, FAIRE enrichment was identified upstream of the constitutively expressed LANA ORF, i.e., at the constitutively active LANA promoter (Fig. 1B). This held true for a second PEL cell line (BC1). To independently confirm the result from BCBL1 cells, we profiled the BC1 cell line in a similar fashion (Fig. 2). The same regions gave rise to prominent sites of FAIRE-seq enrichment. Importantly for FAIRE-seq, as for ChIP-seq data, the peak height is deceiving and cannot be used to infer a linear relationship of abundance (54). We therefore chose to show FAIRE peak region boundaries as boxes beneath the raw data. Open chromatin was observed near the promoter regions of 14 ORFs in BC1, many of which are strongly induced during lytic reactivation, as well as within lytic origins of replication (OriLyt-L or -R) (Fig. 2; Table 2). We were also able to map FAIRE reads to the latent origin of replication, which is located within the terminal repeats (reviewed in reference 19), and this enrichment correlated with previously mapped CTCF and LANA ChIP-seq data (23, 55), as well as *in*

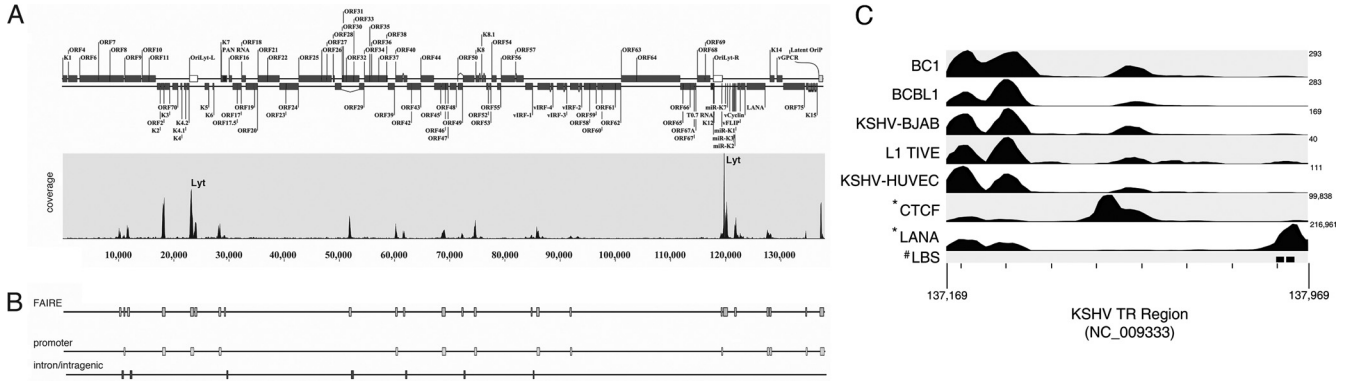

FIG 2 Regions of latent open chromatin across the KSHV genome (BC1). (A) FAIRE-seq reads from BC1 cells mapped to the KSHV reference genome NC_009333 are shown as in Fig. 1. Regions of increased coverage density correspond to regions of KSHV open chromatin. (B) FAIRE peaks in BC1 are identified as blocks and correspond to nucleotide-level resolution latent open chromatin as determined by MACS2. Regions of open chromatin occur in KSHV lytic replication origins (Lyt) and promoter regions and at intronic/intragenic sites during latency. (C) FAIRE-seq coverage of the viral terminal repeat (TR) region of KSHV. CTCF and LANA ChIP-seq enrichments (from GEO data sets GSM941710 and GSM941712, respectively; indicated by asterisks) are included for comparison. LANA binding sites (LBS; indicated by #) in the TR, as determined by Garber et al. (56), are also indicated. Numbers on the right indicate the scale of maximum coverage at the TR region. Nucleotide coordinates are based on NC_009333.

vitro-characterized LANA binding sites (56) (Table 2; Fig. 2C). Every FAIRE site identified corresponded to a previously recognized or predicted regulatory element in the KSHV genome (Table 2).

KSHV exhibits tropism for endothelial and B cell lineages. To expand our observations and to determine if differences in chromatin organization existed among different cell lines and/or among distinct viral isolates, we performed FAIRE-seq on multiple latently infected KSHV cell lines (Fig. 3). The majority of FAIRE-enriched regions were consistently identified across most of the cell lines (see Table S1 in the supplemental material). In

TABLE 2 Correlation between FAIRE peaks in BC1 and other notable chromatin marks

Peak	Region[a]	Size (bp)	"Active"[b]	CTCF[c]	LANA[d]	RTA[e]	Promoter	Description	Reference(s)
1	10083–10467	384	X	X				Intragenic	—[h]
2	10885–11147	262		X			X	ORF8/ORF9	87
3	11567–12002	435		X				Intragenic	—[h]
4[i]	17847–18466	619	X			X[f]	X	vIL6	61
5	22965–23605	640	X	O		X	X	K4.2 OriLyt-L	88, 89
6[i]	23758–24220	462	X			X		OriLyt-L	88, 89
7	28103–28550	447	X	O		X	X	K6/K7/PAN	28, 90
8[i]	29112–29408	296	X		X			Intragenic	9
9	51707–52185	478		X		X		ORF32/ORF29 intron	—[h]
10	60130–60531	401		X			X	ORF39/ORF40-41	—[h]
11	61554–61892	338		X				ORF40-41 intron	—[h]
12	68538–69231	693	X	X		X	X	ORF45	91
13	72133–72463	330		X				ORF50 intron	92
14	74384–74835	451	X	X		X	X	K8	92
15	84695–84973	278	X	X				Intragenic	—[h]
16	85687–86245	558	X	X			X	vIRF1	93
17	91732–92071	339	X	X			X	vIRF3	72
18[i]	119144–119418	274	X			X	X	Kaposin/OriLyt-R	88, 94, 95
19	119546–120371	825	X	O		X	X	OriLyt-R/ALTp	7, 88
20	121573–121961	388	X	X				miR-K12-5. . .miR-K12-2	94, 96
21	127436–127830	394	X	X	X	X	X	LANApi/K14	16, 97, 98
22[i]	127900–128276	376	X				X	LANApc	12
23[i]	134456–134736	280	X		X			5′ ORF75/K15 3′	59, 99
24	137041–137806	765	X	X[g]	X[g]	X	X	K15/TR	100, 101

[a] KSHV reference genome NC_009333.
[b] Distance to histone mark H3K9/K14-ac/H3K4-me3, ≥250 bp, data set S1; see reference 20.
[c] GEO data set GSM941710 (23); X indicates occupation of CTCF and cohesin; O indicates CTCF without cohesin.
[d] GEO data set GSM941712 (23).
[e] See reference 64.
[f] See reference 61.
[g] 35 TR (nt 137169 to 137969 from NC_009333) added to KSHV reference genome HQ404500.1 in GEO data sets GSM941710/GSM941712.
[h] —, data from the work of Russo et al. (102).
[i] Regions of accessible latent chromatin based on FAIRE.

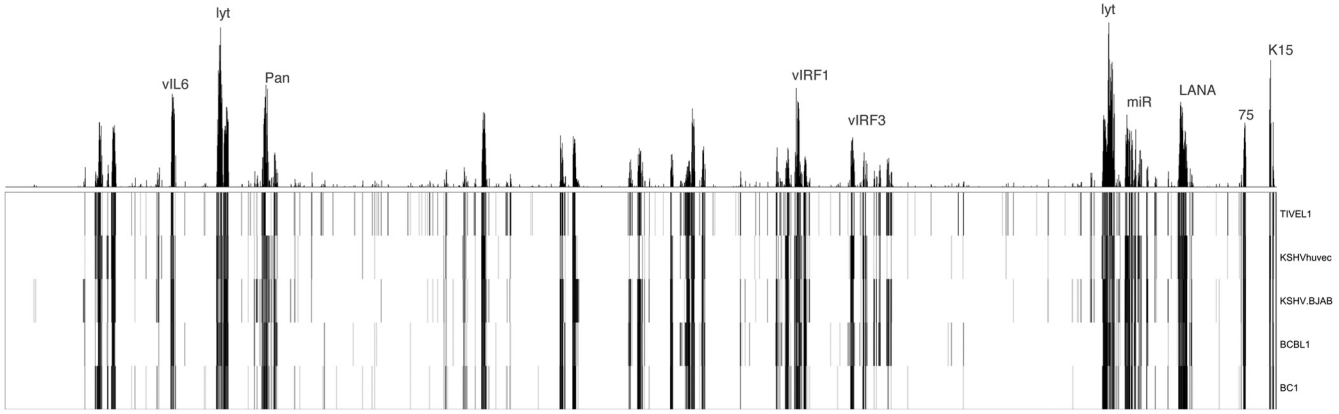

FIG 3 Regions of open chromatin are conserved in latent KSHV-infected endothelial and B cells. A heat map of normalized coverage counts across five cell lines (BC1, BCBL1, BJAB carrying latent KSHV, KSHV-HUVEC carrying latent KSHV, and L1-TIVE cells) is shown. Darker hues indicate nucleosome depletion, i.e., higher FAIRE coverage (averaged over a 40-bp sliding window). On top, the average coverage across all cell lines is shown.

addition, the FAIRE-enriched regions spanning nucleotides (nt) 60180 to 60488 (the presumed bidirectional ORF39/ORF40 promoter), nt 68656 to 69159 (the presumed ORF45 promoter), and nt 121605 to 121917 (within the KSHV miRNA locus in NC_009333) were present only in cell lines of the B cell lineage cell lines, i.e., the PEL lines and the artificially KSHV-infected Burkitt lymphoma cell line KSHV-BJAB, and not in the endothelial cell lines.

Overall, this result supports the notion that during latency in PEL the majority of viral promoters and viral genes are populated by closed chromatin and thus inaccessible to transcription factors and PolII in latent PELs. Twenty-four viral regulatory regions (including some intragenic regions) were identified as open via FAIRE-seq in latent BC1 cells. These included the KSHV latency region, OriLyt-L, and the OriLyt-R, as expected; however, other regions not associated with high levels of latent transcription, but which direct viral early and immediate early lytic transcripts, were also nucleosome depleted. Open chromatin is necessary but not sufficient for transcriptional initiation, and this result suggests that other modulators/marks add transcriptional specificity.

Latent episomal open chromatin is adjacent to activating histone markings. Histones incorporated into the latent KSHV episome display modifications associated with either transcriptionally active or repressed chromatin, except within the viral latency locus (20, 22). To further characterize the KSHV regulatory elements that we identified, we integrated the FAIRE data with ChIP-chip (chromatin immunoprecipitation with microarray technology) data for H3K9-ac, H3K14-ac, and H3K4-me3 (20) (Fig. 4). Specifically, H3K9/K14-ac and/or H3K4-me3 is interpreted to represent an activating histone mark and to demarcate areas associated with active transcription. We used a very stringent cutoff requiring enrichment to be ≥3 standard deviations above a no-signal baseline in data set S1 (20) to determine a significant threshold for these histone modifications, and we then overlaid this enrichment with significant regions of FAIRE-seq-identified viral open chromatin as determined by MACS2. Regions of nucleosome depletion were flanked by these activating histone marks across almost all FAIRE peak regions (data not shown). Eighteen of 24 (~75%) regulatory elements identified by FAIRE-seq in BC1 were within 250 bp (one overlapping tiling window length from reference 20) of regions enriched with H3K9/K14-ac and/or H3K4-me3 histone enrichment (Table 2). For instance, in the OriLyt-L region, open chromatin was found adjacent to H3K4-me3 and H3K9/K14-ac marked nucleosome enrichment (Fig. 4A).

FAIRE-identified nucleosome depletion and H3K4-me3 and H3K9/K14-ac were also in close proximity in the lytic control region (Fig. 4B). Importantly, neither open chromatin nor activating histone marks were found near the RTA/ORF50 promoter. Repressive H3K27-me3 was observed within ORF48 and ORF52. Open chromatin was also detected within the RTA/ORF50 intron. FAIRE enrichment and activating histone modifications were also both detected at the K8 promoter. Lastly, the KSHV latency locus, which as a whole is actively transcribed and subjected to alternative splicing, also showed an expected pattern of open chromatin. We observed increased chromatin accessibility at the LANA promoter, at the OriLyt-R, and across the KSHV miRNA locus (Fig. 4C), which overlapped previously reported H3K4-me3 and/or H3K9/K14-ac-marked nucleosomes. This suggests that these regions are accessible for active transcriptional regulators and/or poised to initiate transcription in response to specific regulators while the virus is in a latent state.

Six FAIRE peaks were not adjacent to activating histone modifications in BC1 (Table 2). Three mapped to introns within ORF29, ORF40/41, and ORF50 (RTA), and three were observed at viral tegument and replication genes, i.e., within the gene body of ORF8 and near the promoter regions of ORF9 and ORF39/40. As expected, no FAIRE enrichment was observed near regions of H3K9-me3, which denotes closed, transcriptionally inactive constitutive heterochromatin. Thus, our experiments using a novel, independent technique verify prior work (20, 22) and the classification of H3K9-me3 as a valuable marker for transcriptionally inactive regions of the latent KSHV genome.

Open chromatin regions overlap CTCF binding sites at inactive promoters. Work by Lieberman and colleagues has shown that interactions between gammaherpesvirus genomes and cellular CTCF/associated cohesins are key regulators of viral gene expression and genome conformation (23, 25, 57, 58). We therefore compared the overlap between regions of nucleosome depletion and that with previously identified CTCF binding sites (23) during KSHV latency using published CTCF ChIP-seq data (data set GSM941710 from reference 23). Eighteen of the 24 (75%) regions

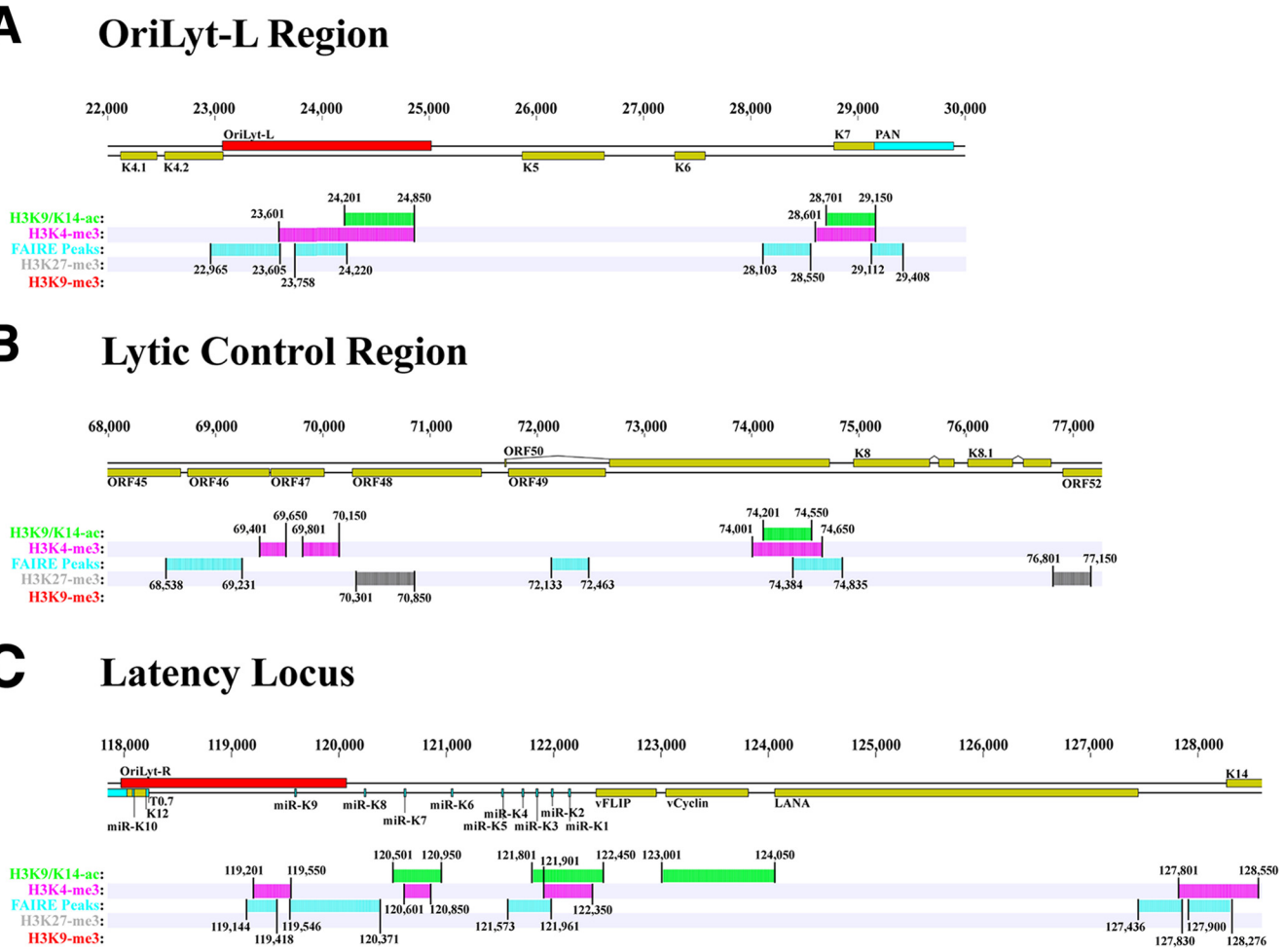

FIG 4 Regions of open chromatin occur near activated histone modifications. Significant regions of overlapping tiled probe enrichment for histone modifications on the latent KSHV genome were annotated from previous work (20). Regions of H3K9/K14-ac and H3K4-me3 activating marks are shown in green and pink, respectively. FAIRE peaks are shown in light blue. H3K27-me3 and H3K9-me3 (not observed at these loci) modifications are shown in gray and red, respectively. The KSHV OriLyt-L region (A), the lytic control region (RTA promoter) (B), and the KSHV latency locus (C) are shown. Nucleotide boundaries in NC_009333 for significant tiled window enrichment from histone ChIP-chip and significant FAIRE-seq enrichment are indicated.

identified by FAIRE-seq overlapped with CTCF binding sites in latently infected BC1 cells (Table 2).

Six regions identified by FAIRE-seq did not demonstrate coincident CTCF binding, suggesting that these regions represent active regulatory scaffolds during latent infection which function independently of CTCF. Two of these regions (one intragenic to the noncoding PAN RNA [9] and one in the 3′ untranscribed region [UTR] of the K15 gene [59]) contained sites which are bound by LANA based on ChIP-seq data (GSM941712 from reference 23) (Table 2). At this point, the functional relevance of LANA binding to these regions is unknown. Given LANA's ability to function as a transactivator if bound to single binding sites outside the terminal repeat (TR) region (which contains multimeric LANA binding sites [60]), one could speculate that these regions may contain yet-to-be-discovered latent promoters.

FAIRE sites lacking CTCF binding occurred within the promoter regions of vIL6 (vIL6p [61]), within the constitutive LANA promoter (LANApc [12]), and upstream of the lytically induced Kaposin promoter (K12p [62]) (Fig. 5). The vIL6 gene is transcribed in otherwise latently infected MCD cells, and K12p expression has been observed during latency (15, 61–65). The vIL6p is strongly activated by RTA but also independently of RTA by the interferon (IFN) signaling pathway and by intracellular Notch (66, 67). These phenotypes are consistent with the presence of the identified open chromatin region in Fig. 5A, which may be regulated by cellular factors independently of the complete replication cycle, and in certain instances independently of RTA.

Another FAIRE site lacking CTCF binding overlapped OriLyt-R, K12p, and the predicted transcription start site (nt ~120544 in NC_009333) of a novel antisense to latent transcripts (ALT) noncoding RNA (7) (Fig. 5B). Hence, it is possible that this region is involved in regulation of three elements: the proximal Kaposin promoter, which is an RTA-responsive early promoter; OriLyt-R accessibility; and the novel ALT promoter. We observed that CTCF binds within open chromatin in the miRK3/K4 locus, a region of abundant latent transcription, but with no known *cis*-regulatory elements (Fig. 5B). Nucleosome depletion devoid of CTCF binding also covered the intergenic region between the LANA ORF and K14 ORF. This region contains known CTCF binding sites downstream of the inducible LANApi; however, the

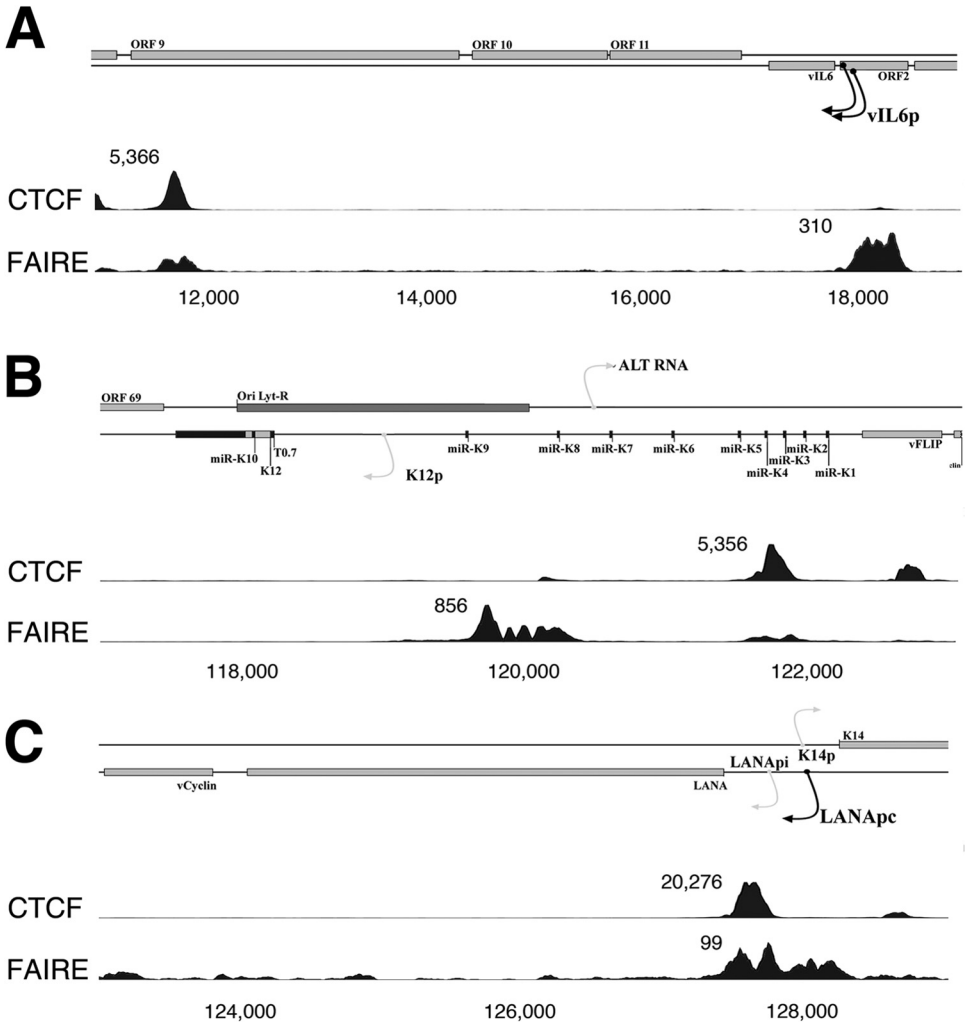

FIG 5 Regions of KSHV open chromatin coincide with CTCF binding sites. The published CTCF ChIP-seq enrichment (GSM941710) (23) is shown in relation to FAIRE-seq coverage. (A) The KSHV genomic region spanning the vIL6p region is shown (nt 11000 to 19000) along with two mapped transcription start sites depicted by black arrows. (B) The approximately mapped transcription start sites for the K12p and the antisense to latent transcripts (ALT) RNA (7) are indicated with gray arrows, and the OriLyt-R is shown (nt 117000 to 123000). (C) The bidirectional transcription start sites for the lytic LANApi and K14p promoters are indicated by gray arrows, and the constitutive LANApc is denoted with a black arrow (nt 123000 to 128000). Note changes in scale between panels. All nucleotide coordinates are based on NC_009333.

constitutive LANApc transcription initiation site was nucleosome depleted (as expected) and was not bound by CTCF (Fig. 5C).

Together, these data suggest that regions of open chromatin in the latent KSHV genome can be divided into two subsets: those which are bound by CTCF and map to transcriptionally inactive loci and are likely regulated by CTCF and those which are not bound by CTCF. The latter include constitutively active or poised promoters, such as LANApc and the Kaposin/OriLyt/ALTp region, and promoters which may be regulated by host factors independently of RTA and KSHV lytic reactivation, such as the vIL6 promoter.

Open chromatin regions overlap RNA polymerase II deposition at active and poised promoters. Toth et al. (28) recently determined latent RNA polymerase II (PolII) occupancy on the KSHV genome. Chen et al. (23) determined the LANA binding sites, which in latent KSHV infection represent another layer of regulation. We thus integrated previously identified PolII binding sites with our set of open chromatin regions. PolII was enriched at the vIL6, vIRF3, LANApc, K4/5/7, K15, and OriLyt regions (Fig. 6A), and these coincided with regions of nucleosome depletion as identified by FAIRE (Fig. 6B). As mentioned above, FAIRE identified many more regions of open chromatin, and the majority of these were bound by CTCF (Fig. 6C), which excluded PolII enrichment to a high degree. LANA bound in the vicinity of CTCF at the OriLyt regions, at the TRs, at the presumed vIRF promoter, and at the inducible LANA promoter but not the constitutively active LANA promoter (Fig. 6D; Table 2).

It is important to recognize the limitations of this type of comparative analysis, which tries to match data from separate experiments, obtained with reagents of differing performance and on different experimental platforms. Array data are normally distributed and have a rather narrow signal-to-noise ratio. ChIP-seq data follow a Poisson distribution. This type of distribution is highly nonlinear and tends to overemphasize peaks (54). To compare

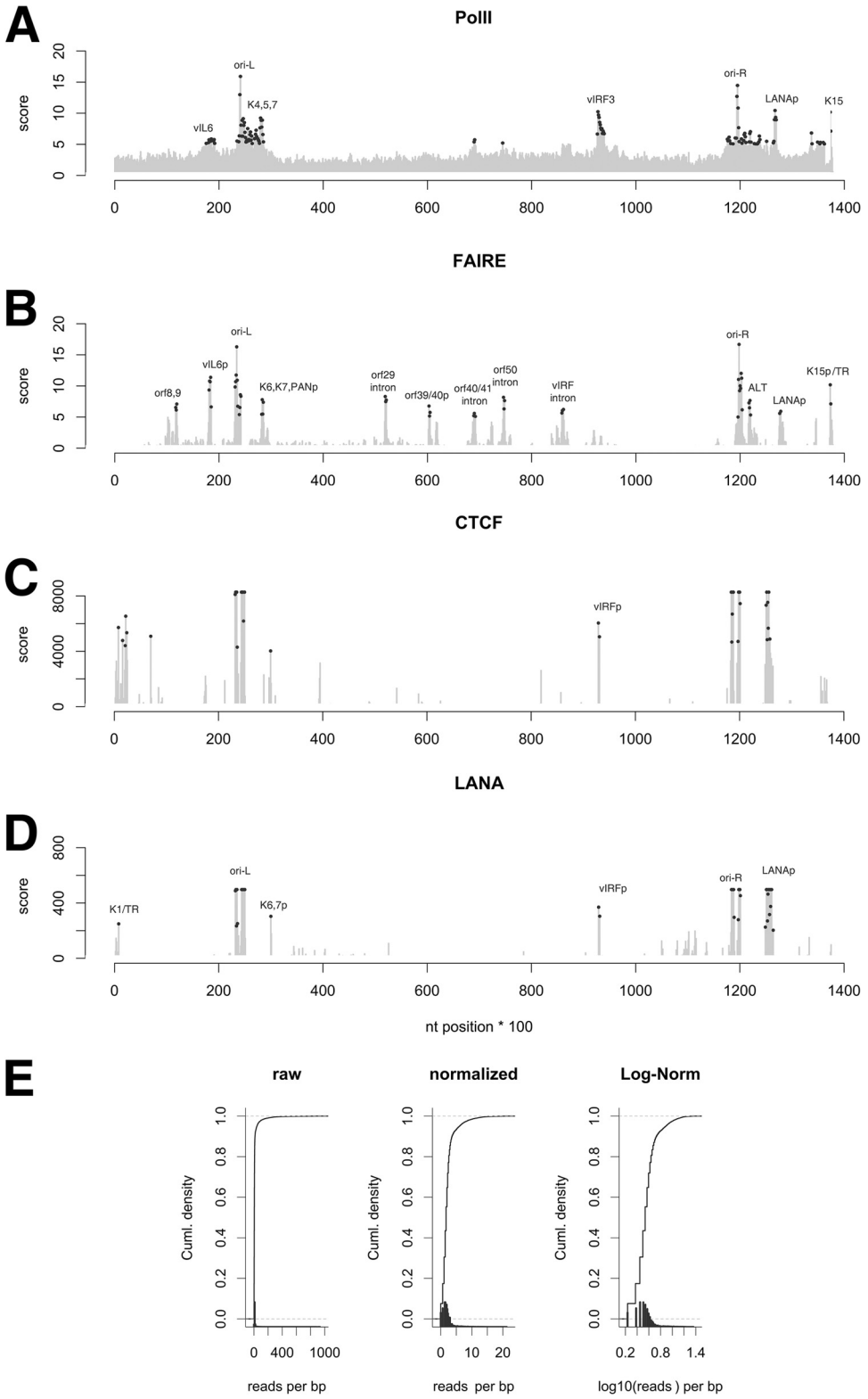

FIG 6 RNA PolII designates KSHV latent promoters. (A to D) Comparison of PolII (A), FAIRE (B), CTCF (C), and LANA (D) enrichment across the KSHV genome. The horizontal axis represents the genome location; the vertical axis represents the relative enrichment score over a 100-bp sliding window. Dots indicate significant peaks. (E) Normalization process. Shown on the horizontal axis is the unit and on the vertical axis is the cumulative density. Data are shown as deep sequence-derived coverage counts (raw), normalized counts $\{[n^{1/3} - \text{median}\,(n^{1/3})]/(\text{interquartile range}\ n^{1/3}/1.349)\}$, and $\log_{10}$ of normalized counts, which are approximately normally distributed.

these different data sets, we applied successive transformation steps to facilitate the comparison between array and ChIP-seq data sets (Fig. 6E). This is necessary to take into account the different data structures of each experiment. Specifically, the ChIP-chip data (Fig. 6A) follow an approximately normal distribution, whereas raw ChIP-seq and FAIRE data follow a Poisson or negative binomial distribution. Each of these transformations incurs some loss of resolution, but they are necessary in order to make a justified comparison. Figure 6E plots the cumulative signal intensity per base pair. As can be seen after normalizing and logarithmic transformation, the ChIP-seq data are normally distributed, making formal comparisons possible. Collectively, these data support the general conclusion of a layered model, in which each of the layers (nucleosome position, histone marks, methylation, CTCF, and LANA) contributes to the final signal, which is PolII recruitment and productive transcription.

DISCUSSION

The goal of this study was to investigate chromatin organization of KSHV during latency. It follows our prior work mapping KSHV mRNA and miRNA transcription (68, 69). Only two regions of the genome were previously known to be consistently transcribed in latently infected cells: the KSHV latency locus (encoding LANA, vCYC, vFLIP, Kaposin/K12, and all viral miRNAs) and vIRF3/LANA-2 (12, 70). More recently, evidence for more widespread viral transcription has emerged. The vIL6 gene is expressed at high levels in MCD and can respond to alpha interferon (IFN-α) independently of other viral genes (67, 71). For vIRF1, both a latent and a lytic transcription start site have been described (72), and we previously detected vIRF1 mRNA in KS lesions (73). Similarly, K1 was widely expressed in at least a subset of KS tumors (74). No significant FAIRE enrichment was observed near the K1 locus in our experiments. We speculate that this may be due to differences in the microenvironment or the inherent propensity of FAIRE to record the majority occupancy state. FAIRE (and for that matter all epigenetic profiling approaches with the exception of MAPit [52]) requires 10^6 or more cells of similar epigenetic status to record a signal. In contrast, we estimate that we can detect one K1 mRNA-expressing cell in a background of 10,000 non-K1-expressing cells. Lastly, genomic surveys found extensive transcription, including the expression of noncoding RNAs, across the entire genome (7, 8, 75). We hypothesized that mapping open chromatin, which is a prerequisite for transcription, may yield further insights and would allow us to classify KSHV *cis* elements into different groups, based on their epigenetic status during latency.

We are not the first to investigate the viral epigenome (reviewed in reference 4). Extensive studies by many groups determined the KSHV CpG methylation status and modified histone deposition across the genome (20, 22, 76). We were able to integrate this information using FAIRE (32, 35) as a novel method to further characterize the chromatin status in KSHV. The open chromatin regions identified by FAIRE can be thought of as a minimal requirement for epigenetic and/or transcriptional regulation (reviewed in reference 77). Modified histone marks and transcription factor occupancy binding represent the next layer, and subsequent PolII recruitment and successful elongation each contribute to the final level of transcriptional regulation. One way to think about the extensive epigenetic information that has been generated for KSHV is as tiered arrangements of safety locks; each lock has to be opened before a transcript is produced. The first layer of access is at the nucleosome level. Only sites that are nucleosome depleted can engage transcription factors. These are identifiable by FAIRE. The next layer of access is at the histone-code level. Only regions enriched in activating histone marks are likely to engage transcription factors. An additional regulatory safeguard here is CTCF, which marks open chromatin regions at viral loci, which are conventionally transcriptionally inactive during latency. The final layer is recruitment of RNA PolII and its activation via C-terminal domain (CTD) modification.

We found that regions of open chromatin decorated ~8% of the latent BC1 genome, meaning that most of the KSHV genome was occupied by nucleosomes during latency. This is consistent with prior work by Günther and Grundhoff which also demonstrated genome-wide CpG DNA methylation (20). Closed chromatin, as ascertained by lack of a significant FAIRE peak, also correlated (within the limit of ChIP-chip) well with repressive histone marks H3K9-me3 and H3K27-me3, as well as with binding sites for EZH2, the enzymatic component of the complex responsible for H3K27-me3, as reported by Toth et al. (22) and also by Grundhoff and others (20, 21, 23). A few open chromatin regions mapped to KSHV intronic and intragenic loci. At this point, we do not know the significance of this observation, which has been noted in other studies using FAIRE and attributed, for instance, to altered nucleosome organization around splice sites and/or introns (38, 43, 78). These are unlikely to be novel latent promoters, since they were notably devoid of proximal H3K9/K14-ac or H3K4-me3 enrichment.

We found 24 sites of open chromatin in the latent KSHV genome in BC1 (Table 2). These lacked repressive histone marks and were in close proximity to previously reported (20) histone modifications associated with transcriptional activity (H3K4-me3 and H3K9/K14-ac). These 24 regions of open chromatin could be further subdivided on the basis of CTCF co-occupancy as determined by Chen et al. and others (21, 23–27).

The constitutive LANA promoter (LANApc), the vIL6 promoter, and the proximal Kaposin/presumed promoter for the ALT transcript represent open chromatin regions not co-occupied by CTCF. Nearly all other regions of nucleosome depletion contained previously reported CTCF binding sites; which we presume modulate the transcriptional utility of these regions (23). CTCF has a predominantly insulating, albeit dynamic and variable, role at cellular loci (reviewed in references 79, 80, and 81). CTCF modulates latent gene regulation and episomal configuration in both human gammaherpesviruses (23, 25, 26, 82–86); thus, CTCF-mediated regulation represents a mechanism that may control the transcriptional usage of KSHV episomal regulatory scaffolds during latent infection. Eleven of 24 (46%) latent regions of open chromatin also localized to known binding sites for the KSHV lytic switch protein RTA (61, 64) (Table 2), suggesting that latent regions of nucleosome depletion may also require RTA expression for regulatory function.

The nucleosome depletion pattern was highly conserved among multiple cells with stably and latently maintained KSHV episomes. PEL cell lines and artificially KSHV-infected BJAB cells yielded largely superimposable FAIRE profiles. Two endothelial lineage models of latent KSHV infection (L1-TIVE [46] and KSHV-HUVEC [47]) also shared many of the same regions of open chromatin with B cells. However, we also identified B-cell-

specific regions of open chromatin, which are the subject of further study.

Lastly, we integrated our FAIRE data with LANA binding sites from the work of Chen et al. (23) (GSM941712) and RNA PolIII data from the work of Toth et al. (28). This indicated that the regions with a high level of association with RNA PolII were indeed the extended KSHV latency locus, the vIRF3 locus, and regions on either side of each OriLyt and that these were bordered by regions of open chromatin. There were fewer PolII peaks than FAIRE peaks, as expected. Additional suppressive mechanisms during latency may arise from negative elongation factor (NELF)-mediated PolII stalling, which has been characterized in KSHV, such as within the region spanning OriLyt-L to K7 (28).

In sum, FAIRE-seq represents a robust method, perhaps more so than antibody-dependent ChIP-seq, to identify regions of open chromatin with single-nucleotide resolution. We applied this method for the first time to identify regions of open chromatin in the latent KSHV genome and identified several regions of open chromatin in latent viral episomes. Nucleosome depletion alone is not sufficient to predict regions of active latent transcription; however, by integrating prior data on histone modifications, as well as binding sites for LANA, PolII, and CTCF, we generated a genome-wide map of the latent KSHV chromatin landscape. This effort is in concordance with transcriptional profiling and suggests the presence of additional latent regulatory regions in the viral genome.

ACKNOWLEDGMENTS

We thank the UNC High-Throughput Sequencing Facility and UNC Vironomics core.

This work was supported by NIH grants CA109232 and AI107810 to D.P.D., CA019014 to B.D., CA166447 to I.J.D., T32GM067553 to J.M.S., and T32AI007419 to I.B.H.

REFERENCES

1. **Chang Y, Cesarman E, Pessin MS, Lee F, Culpepper J, Knowles DM, Moore PS.** 1994. Identification of herpesvirus-like DNA sequences in AIDS-associated Kaposi's sarcoma. Science **266:**1865–1869.
2. **Cesarman E, Chang Y, Moore PS, Said JW, Knowles DM.** 1995. Kaposi's sarcoma-associated herpesvirus-like DNA sequences in AIDS-related body-cavity-based lymphomas. N. Engl. J. Med. **332:**1186–1191.
3. **Soulier J, Grollet L, Oksenhendler E, Cacoub P, Cazals-Hatem D, Babinet P, d'Agay MF, Clauvel JP, Raphael M, Degos L, Sigaux F.** 1995. Kaposi's sarcoma-associated herpesvirus-like DNA sequences in multicentric Castleman's disease. Blood **86:**1276–1280.
4. **Knipe DM, Lieberman PM, Jung JU, McBride AA, Morris KV, Ott M, Margolis D, Nieto A, Nevels M, Parks RJ, Kristie TM.** 2013. Snapshots: chromatin control of viral infection. Virology **435:**141–156.
5. **Mesri EA, Cesarman E, Boshoff C.** 2010. Kaposi's sarcoma and its associated herpesvirus. Nat. Rev. Cancer **10:**707–719.
6. **Speck SH, Ganem D.** 2010. Viral latency and its regulation: lessons from the gamma-herpesviruses. Cell Host Microbe **8:**100–115.
7. **Chandriani S, Xu Y, Ganem D.** 2010. The lytic transcriptome of Kaposi's sarcoma-associated herpesvirus reveals extensive transcription of noncoding regions, including regions antisense to important genes. J. Virol. **84:**7934–7942.
8. **Dresang LR, Teuton JR, Feng H, Jacobs JM, Camp DG, II, Purvine SO, Gritsenko MA, Li Z, Smith RD, Sugden B, Moore PS, Chang Y.** 2011. Coupled transcriptome and proteome analysis of human lymphotropic tumor viruses: insights on the detection and discovery of viral genes. BMC Genomics **12:**625. doi:10.1186/1471-2164-12-625.
9. **Sun R, Lin SF, Gradoville L, Miller G.** 1996. Polyadenylylated nuclear RNA encoded by Kaposi sarcoma-associated herpesvirus. Proc. Natl. Acad. Sci. U. S. A. **93:**11883–11888.
10. **Cullen BR.** 2006. Viruses and microRNAs. Nat. Genet. **38**(Suppl):S25–S30.
11. **Zheng ZM.** 2010. Viral oncogenes, noncoding RNAs, and RNA splicing in human tumor viruses. Int. J. Biol. Sci. **6:**730–755.
12. **Dittmer D, Lagunoff M, Renne R, Staskus K, Haase A, Ganem D.** 1998. A cluster of latently expressed genes in Kaposi's sarcoma-associated herpesvirus. J. Virol. **72:**8309–8315.
13. **Sarid R, Wiezorek JS, Moore PS, Chang Y.** 1999. Characterization and cell cycle regulation of the major Kaposi's sarcoma-associated herpesvirus (human herpesvirus 8) latent genes and their promoter. J. Virol. **73:**1438–1446.
14. **Talbot SJ, Weiss RA, Kellam P, Boshoff C.** 1999. Transcriptional analysis of human herpesvirus-8 open reading frames 71, 72, 73, K14, and 74 in a primary effusion lymphoma cell line. Virology **257:**84–94.
15. **Cai X, Cullen BR.** 2006. Transcriptional origin of Kaposi's sarcoma-associated herpesvirus microRNAs. J. Virol. **80:**2234–2242.
16. **Hilton IB, Dittmer DP.** 2012. Quantitative analysis of the bidirectional viral G-protein-coupled receptor and lytic latency-associated nuclear antigen promoter of Kaposi's sarcoma-associated herpesvirus. J. Virol. **86:**9683–9695.
17. **Kedes DH, Lagunoff M, Renne R, Ganem D.** 1997. Identification of the gene encoding the major latency-associated nuclear antigen of the Kaposi's sarcoma-associated herpesvirus. J. Clin. Invest. **100:**2606–2610.
18. **Rainbow L, Platt GM, Simpson GR, Sarid R, Gao SJ, Stoiber H, Herrington CS, Moore PS, Schulz TF.** 1997. The 222- to 234-kilodalton latent nuclear protein (LNA) of Kaposi's sarcoma-associated herpesvirus (human herpesvirus 8) is encoded by orf73 and is a component of the latency-associated nuclear antigen. J. Virol. **71:**5915–5921.
19. **Ballestas ME, Kaye KM.** 2011. The latency-associated nuclear antigen, a multifunctional protein central to Kaposi's sarcoma-associated herpesvirus latency. Future Microbiol. **6:**1399–1413.
20. **Gunther T, Grundhoff A.** 2010. The epigenetic landscape of latent Kaposi sarcoma-associated herpesvirus genomes. PLoS Pathog. **6:**e1000935. doi:10.1371/journal.ppat.1000935.
21. **Stedman W, Deng Z, Lu F, Lieberman PM.** 2004. ORC, MCM, and histone hyperacetylation at the Kaposi's sarcoma-associated herpesvirus latent replication origin. J. Virol. **78:**12566–12575.
22. **Toth Z, Maglinte DT, Lee SH, Lee HR, Wong LY, Brulois KF, Lee S, Buckley JD, Laird PW, Marquez VE, Jung JU.** 2010. Epigenetic analysis of KSHV latent and lytic genomes. PLoS Pathog. **6:**e1001013. doi:10.1371/journal.ppat.1001013.
23. **Chen HS, Wikramasinghe P, Showe L, Lieberman PM.** 2012. Cohesins repress Kaposi's sarcoma-associated herpesvirus immediate early gene transcription during latency. J. Virol. **86:**9454–9464.
24. **Kang H, Cho H, Sung GH, Lieberman PM.** 2013. CTCF regulates Kaposi's sarcoma-associated herpesvirus latency transcription by nucleosome displacement and RNA polymerase programming. J. Virol. **87:**1789–1799.
25. **Kang H, Lieberman PM.** 2009. Cell cycle control of Kaposi's sarcoma-associated herpesvirus latency transcription by CTCF-cohesin interactions. J. Virol. **83:**6199–6210.
26. **Kang H, Wiedmer A, Yuan Y, Robertson E, Lieberman PM.** 2011. Coordination of KSHV latent and lytic gene control by CTCF-cohesin mediated chromosome conformation. PLoS Pathog. **7:**e1002140. doi:10.1371/journal.ppat.1002140.
27. **Stedman W, Kang H, Lin S, Kissil JL, Bartolomei MS, Lieberman PM.** 2008. Cohesins localize with CTCF at the KSHV latency control region and at cellular c-myc and H19/Igf2 insulators. EMBO J. **27:**654–666.
28. **Toth Z, Brulois KF, Wong LY, Lee HR, Chung B, Jung JU.** 2012. Negative elongation factor-mediated suppression of RNA polymerase II elongation of Kaposi's sarcoma-associated herpesvirus lytic gene expression. J. Virol. **86:**9696–9707.
29. **Boyle AP, Davis S, Shulha HP, Meltzer P, Margulies EH, Weng Z, Furey TS, Crawford GE.** 2008. High-resolution mapping and characterization of open chromatin across the genome Cell **132:**311–322.
30. **Gross DS, Garrard WT.** 1988. Nuclease hypersensitive sites in chromatin. Annu. Rev. Biochem. **57:**159–197.
31. **Song L, Crawford GE.** 2010. DNase-seq: a high-resolution technique for mapping active gene regulatory elements across the genome from mammalian cells. Cold Spring Harbor Protoc. **2010**(2):pdb.prot5384. doi:10.1101/pdb.prot5384.
32. **Giresi PG, Lieb JD.** 2009. Isolation of active regulatory elements from eukaryotic chromatin using FAIRE (Formaldehyde Assisted Isolation of Regulatory Elements). Methods **48:**233–239.
33. **Hogan GJ, Lee CK, Lieb JD.** 2006. Cell cycle-specified fluctuation of

nucleosome occupancy at gene promoters. PLoS Genet. **2:**e158. doi:10.1371/journal.pgen.0020158.
34. **Nagy PL, Cleary ML, Brown PO, Lieb JD.** 2003. Genomewide demarcation of RNA polymerase II transcription units revealed by physical fractionation of chromatin. Proc. Natl. Acad. Sci. U. S. A. **100:**6364–6369.
35. **Simon JM, Giresi PG, Davis IJ, Lieb JD.** 2012. Using formaldehyde-assisted isolation of regulatory elements (FAIRE) to isolate active regulatory DNA. Nat. Protoc. **7:**256–267.
36. **Calabrese JM, Sun W, Song L, Mugford JW, Williams L, Yee D, Starmer J, Mieczkowski P, Crawford GE, Magnuson T.** 2012. Site-specific silencing of regulatory elements as a mechanism of X inactivation. Cell **151:**951–963.
37. **ENCODE Project Consortium, Bernstein BE, Birney E, Dunham I, Green ED, Gunter C, Snyder M.** 2012. An integrated encyclopedia of DNA elements in the human genome. Nature **489:**57–74.
38. **Gaulton KJ, Nammo T, Pasquali L, Simon JM, Giresi PG, Fogarty MP, Panhuis TM, Mieczkowski P, Secchi A, Bosco D, Berney T, Montanya E, Mohlke KL, Lieb JD, Ferrer J.** 2010. A map of open chromatin in human pancreatic islets. Nat. Genet. **42:**255–259.
39. **Giresi PG, Kim J, McDaniell RM, Iyer VR, Lieb JD.** 2007. FAIRE (Formaldehyde-Assisted Isolation of Regulatory Elements) isolates active regulatory elements from human chromatin. Genome Res. **17:**877–885.
40. **Nitzsche A, Paulus C, Nevels M.** 2008. Temporal dynamics of cytomegalovirus chromatin assembly in productively infected human cells. J. Virol. **82:**11167–11180.
41. **Ponts N, Harris EY, Prudhomme J, Wick I, Eckhardt-Ludka C, Hicks GR, Hardiman G, Lonardi S, Le Roch KG.** 2010. Nucleosome landscape and control of transcription in the human malaria parasite. Genome Res. **20:**228–238.
42. **Rossetto CC, Tarrant-Elorza M, Pari GS.** 2013. Cis and trans acting factors involved in human cytomegalovirus experimental and natural latent infection of CD14 (+) monocytes and CD34 (+) cells. PLoS Pathog. **9:**e1003366. doi:10.1371/journal.ppat.1003366.
43. **Song L, Zhang Z, Grasfeder LL, Boyle AP, Giresi PG, Lee BK, Sheffield NC, Graf S, Huss M, Keefe D, Liu Z, London D, McDaniell RM, Shibata Y, Showers KA, Simon JM, Vales T, Wang T, Winter D, Clarke ND, Birney E, Iyer VR, Crawford GE, Lieb JD, Furey TS.** 2011. Open chromatin defined by DNaseI and FAIRE identifies regulatory elements that shape cell-type identity. Genome Res. **21:**1757–1767.
44. **Roy D, Sin SH, Damania B, Dittmer DP.** 2011. Tumor suppressor genes FHIT and WWOX are deleted in primary effusion lymphoma (PEL) cell lines. Blood **118:**e32–e39. doi:10.1182/blood-2010-12-323659.
45. **Nun TK, Kroll DJ, Oberlies NH, Soejarto DD, Case RJ, Piskaut P, Matainaho T, Hilscher C, Wang L, Dittmer DP, Gao SJ, Damania B.** 2007. Development of a fluorescence-based assay to screen antiviral drugs against Kaposi's sarcoma associated herpesvirus. Mol. Cancer Ther. **6:**2360–2370.
46. **An FQ, Folarin HM, Compitello N, Roth J, Gerson SL, McCrae KR, Fakhari FD, Dittmer DP, Renne R.** 2006. Long-term-infected telomerase-immortalized endothelial cells: a model for Kaposi's sarcoma-associated herpesvirus latency in vitro and in vivo. J. Virol. **80:**4833–4846.
47. **Wang L, Damania B.** 2008. Kaposi's sarcoma-associated herpesvirus confers a survival advantage to endothelial cells. Cancer Res. **68:**4640–4648.
48. **Lassmann T, Hayashizaki Y, Daub CO.** 2009. TagDust—a program to eliminate artifacts from next generation sequencing data. Bioinformatics **25:**2839–2840.
49. **Langmead B, Trapnell C, Pop M, Salzberg SL.** 2009. Ultrafast and memory-efficient alignment of short DNA sequences to the human genome. Genome Biol. **10:**R25. doi:10.1186/gb-2009-10-3-r25.
50. **Feng J, Liu T, Qin B, Zhang Y, Liu XS.** 2012. Identifying ChIP-seq enrichment using MACS. Nat. Protoc. **7:**1728–1740.
51. **Renne R, Zhong W, Herndier B, McGrath M, Abbey N, Kedes D, Ganem D.** 1996. Lytic growth of Kaposi's sarcoma-associated herpesvirus (human herpesvirus 8) in culture. Nat. Med. **2:**342–346.
52. **Darst RP, Haecker I, Pardo CE, Renne R, Kladde MP.** 2013. Epigenetic diversity of Kaposi's sarcoma-associated herpesvirus. Nucleic Acids Res. **41:**2993–3009.
53. **Tamburro KM, Yang D, Poisson J, Fedoriw Y, Roy D, Lucas A, Sin SH, Malouf N, Moylan V, Damania B, Moll S, van der Horst C, Dittmer DP.** 2012. Vironome of Kaposi sarcoma associated herpesvirus-inflammatory cytokine syndrome in an AIDS patient reveals co-infection of human herpesvirus 8 and human herpesvirus 6A. Virology **433:**220–225.
54. **Lee S, Chugh PE, Shen H, Eberle RW, Dittmer DP.** 2013. Poisson factor models with applications to non-normalized microRNA profiling. Bioinformatics **29:**1105–1111.
55. **Lu F, Tsai K, Chen HS, Wikramasinghe P, Davuluri RV, Showe L, Domsic J, Marmorstein R, Lieberman PM.** 2012. Identification of host-chromosome binding sites and candidate gene targets for Kaposi's sarcoma-associated herpesvirus LANA. J. Virol. **86:**5752–5762.
56. **Garber AC, Hu J, Renne R.** 2002. Latency-associated nuclear antigen (LANA) cooperatively binds to two sites within the terminal repeat, and both sites contribute to the ability of LANA to suppress transcription and to facilitate DNA replication. J. Biol. Chem. **277:**27401–27411.
57. **Chau CM, Zhang XY, McMahon SB, Lieberman PM.** 2006. Regulation of Epstein-Barr virus latency type by the chromatin boundary factor CTCF. J. Virol. **80:**5723–5732.
58. **Tempera I, Klichinsky M, Lieberman PM.** 2011. EBV latency types adopt alternative chromatin conformations. PLoS Pathog. **7:**e1002180. doi:10.1371/journal.ppat.1002180.
59. **Glenn M, Rainbow L, Aurade F, Davison A, Schulz TF.** 1999. Identification of a spliced gene from Kaposi's sarcoma-associated herpesvirus encoding a protein with similarities to latent membrane proteins 1 and 2A of Epstein-Barr virus. J. Virol. **73:**6953–6963.
60. **Jeong JH, Orvis J, Kim JW, McMurtrey CP, Renne R, Dittmer DP.** 2004. Regulation and autoregulation of the promoter for the latency-associated nuclear antigen of Kaposi's sarcoma-associated herpesvirus. J. Biol. Chem. **279:**16822–16831.
61. **Deng H, Song MJ, Chu JT, Sun R.** 2002. Transcriptional regulation of the interleukin-6 gene of human herpesvirus 8 (Kaposi's sarcoma-associated herpesvirus). J. Virol. **76:**8252–8264.
62. **Sadler R, Wu L, Forghani B, Renne R, Zhong W, Herndier B, Ganem D.** 1999. A complex translational program generates multiple novel proteins from the latently expressed kaposin (K12) locus of Kaposi's sarcoma-associated herpesvirus. J. Virol. **73:**5722–5730.
63. **Chandriani S, Ganem D.** 2010. Array-based transcript profiling and limiting-dilution reverse transcription-PCR analysis identify additional latent genes in Kaposi's sarcoma-associated herpesvirus. J. Virol. **84:**5565–5573.
64. **Chen J, Ye F, Xie J, Kuhne K, Gao SJ.** 2009. Genome-wide identification of binding sites for Kaposi's sarcoma-associated herpesvirus lytic switch protein, RTA. Virology **386:**290–302.
65. **Nicholas J, Ruvolo VR, Burns WH, Sandford G, Wan X, Ciufo D, Hendrickson SB, Guo HG, Hayward GS, Reitz MS.** 1997. Kaposi's sarcoma-associated human herpesvirus-8 encodes homologues of macrophage inflammatory protein-1 and interleukin-6. Nat. Med. **3:**287–292.
66. **Chang H, Dittmer DP, Shin YC, Hong Y, Jung JU.** 2005. Role of Notch signal transduction in Kaposi's sarcoma-associated herpesvirus gene expression. J. Virol. **79:**14371–14382.
67. **Chatterjee M, Osborne J, Bestetti G, Chang Y, Moore PS.** 2002. Viral IL-6-induced cell proliferation and immune evasion of interferon activity. Science **298:**1432–1435.
68. **Fakhari FD, Dittmer DP.** 2002. Charting latency transcripts in Kaposi's sarcoma-associated herpesvirus by whole-genome real-time quantitative PCR. J. Virol. **76:**6213–6223.
69. **O'Hara AJ, Chugh P, Wang L, Netto EM, Luz E, Harrington WJ, Dezube BJ, Damania B, Dittmer DP.** 2009. Pre-micro RNA signatures delineate stages of endothelial cell transformation in Kaposi sarcoma. PLoS Pathog. **5:**e1000389. doi:10.1371/journal.ppat.1000389.
70. **Rivas C, Thlick AE, Parravicini C, Moore PS, Chang Y.** 2001. Kaposi's sarcoma-associated herpesvirus LANA2 is a B-cell-specific latent viral protein that inhibits p53. J. Virol. **75:**429–438.
71. **Aoki Y, Tosato G, Fonville TW, Pittaluga S.** 2001. Serum viral interleukin-6 in AIDS-related multicentric Castleman disease. Blood **97:**2526–2527.
72. **Cunningham C, Barnard S, Blackbourn DJ, Davison AJ.** 2003. Transcription mapping of human herpesvirus 8 genes encoding viral interferon regulatory factors. J. Gen. Virol. **84:**1471–1483.
73. **Dittmer DP.** 2003. Transcription profile of Kaposi's sarcoma-associated herpesvirus in primary Kaposi's sarcoma lesions as determined by real-time PCR arrays. Cancer Res. **63:**2010–2015.

74. **Wang L, Dittmer DP, Tomlinson CC, Fakhari FD, Damania B.** 2006. Immortalization of primary endothelial cells by the K1 protein of Kaposi's sarcoma-associated herpesvirus. Cancer Res. **66:**3658–3666.
75. **Xu Y, Ganem D.** 2010. Making sense of antisense: seemingly noncoding RNAs antisense to the master regulator of Kaposi's sarcoma-associated herpesvirus lytic replication do not regulate that transcript but serve as mRNAs encoding small peptides. J. Virol. **84:**5465–5475.
76. **Kati S, Tsao EH, Gunther T, Weidner-Glunde M, Rothamel T, Grundhoff A, Kellam P, Schulz TF.** 2013. Activation of the B cell antigen receptor triggers reactivation of latent Kaposi's sarcoma-associated herpesvirus in B cells. J. Virol. **87:**8004–8016.
77. **Jiang C, Pugh BF.** 2009. Nucleosome positioning and gene regulation: advances through genomics. Nat. Rev. Genet. **10:**161–172.
78. **Wilhelm BT, Marguerat S, Aligianni S, Codlin S, Watt S, Bahler J.** 2011. Differential patterns of intronic and exonic DNA regions with respect to RNA polymerase II occupancy, nucleosome density and H3K36me3 marking in fission yeast. Genome Biol. **12:**R82. doi:10.1186/gb-2011-12-8-r82.
79. **Merkenschlager M.** 2010. Cohesin: a global player in chromosome biology with local ties to gene regulation. Curr. Opin. Genet. Dev. **20:**555–561.
80. **Ohlsson R, Bartkuhn M, Renkawitz R.** 2010. CTCF shapes chromatin by multiple mechanisms: the impact of 20 years of CTCF research on understanding the workings of chromatin. Chromosoma **119:**351–360.
81. **Phillips JE, Corces VG.** 2009. CTCF: master weaver of the genome. Cell **137:**1194–1211.
82. **Chau CM, Lieberman PM.** 2004. Dynamic chromatin boundaries delineate a latency control region of Epstein-Barr virus. J. Virol. **78:**12308–12319.
83. **Holdorf MM, Cooper SB, Yamamoto KR, Miranda JJ.** 2011. Occupancy of chromatin organizers in the Epstein-Barr virus genome. Virology **415:**1–5.
84. **Hughes DJ, Marendy EM, Dickerson CA, Yetming KD, Sample CE, Sample JT.** 2012. Contributions of CTCF and DNA methyltransferases DNMT1 and DNMT3B to Epstein-Barr virus restricted latency. J. Virol. **86:**1034–1045.
85. **Tempera I, Lieberman PM.** 2010. Chromatin organization of gammaherpesvirus latent genomes. Biochim. Biophys. Acta **1799:**236–245.
86. **Tempera I, Wiedmer A, Dheekollu J, Lieberman PM.** 2010. CTCF prevents the epigenetic drift of EBV latency promoter Qp. PLoS Pathog. **6:**e1001048. doi:10.1371/journal.ppat.1001048.
87. **Lin K, Dai CY, Ricciardi RP.** 1998. Cloning and functional analysis of Kaposi's sarcoma-associated herpesvirus DNA polymerase and its processivity factor. J. Virol. **72:**6228–6232.
88. **Lin CL, Li H, Wang Y, Zhu FX, Kudchodkar S, Yuan Y.** 2003. Kaposi's sarcoma-associated herpesvirus lytic origin (ori-Lyt)-dependent DNA replication: identification of the ori-Lyt and association of K8 bZip protein with the origin. J. Virol. **77:**5578–5588.
89. **Wang Y, Li H, Chan MY, Zhu FX, Lukac DM, Yuan Y.** 2004. Kaposi's sarcoma-associated herpesvirus ori-Lyt-dependent DNA replication: *cis*-acting requirements for replication and ori-Lyt-associated RNA transcription. J. Virol. **78:**8615–8629.
90. **Song MJ, Brown HJ, Wu TT, Sun R.** 2001. Transcription activation of polyadenylated nuclear RNA by RTA in human herpesvirus 8/Kaposi's sarcoma-associated herpesvirus. J. Virol. **75:**3129–3140.
91. **Zhu FX, Cusano T, Yuan Y.** 1999. Identification of the immediate-early transcripts of Kaposi's sarcoma-associated herpesvirus. J. Virol. **73:**5556–5567.
92. **Lukac DM, Kirshner JR, Ganem D.** 1999. Transcriptional activation by the product of open reading frame 50 of Kaposi's sarcoma-associated herpesvirus is required for lytic viral reactivation in B cells. J. Virol. **73:**9348–9361.
93. **Chen J, Ueda K, Sakakibara S, Okuno T, Yamanishi K.** 2000. Transcriptional regulation of the Kaposi's sarcoma-associated herpesvirus viral interferon regulatory factor gene. J. Virol. **74:**8623–8634.
94. **Cai X, Lu S, Zhang Z, Gonzalez CM, Damania B, Cullen BR.** 2005. Kaposi's sarcoma-associated herpesvirus expresses an array of viral microRNAs in latently infected cells. Proc. Natl. Acad. Sci. U. S. A. **102:**5570–5575.
95. **Li H, Komatsu T, Dezube BJ, Kaye KM.** 2002. The Kaposi's sarcoma-associated herpesvirus K12 transcript from a primary effusion lymphoma contains complex repeat elements, is spliced, and initiates from a novel promoter. J. Virol. **76:**11880–11888.
96. **Samols MA, Hu J, Skalsky RL, Renne R.** 2005. Cloning and identification of a microRNA cluster within the latency-associated region of Kaposi's sarcoma-associated herpesvirus. J. Virol. **79:**9301–9305.
97. **Kirshner JR, Staskus K, Haase A, Lagunoff M, Ganem D.** 1999. Expression of the open reading frame 74 (G-protein-coupled receptor) gene of Kaposi's sarcoma (KS)-associated herpesvirus: implications for KS pathogenesis. J. Virol. **73:**6006–6014.
98. **Matsumura S, Fujita Y, Gomez E, Tanese N, Wilson AC.** 2005. Activation of the Kaposi's sarcoma-associated herpesvirus major latency locus by the lytic switch protein RTA (ORF50). J. Virol. **79:**8493–8505.
99. **Poole LJ, Zong JC, Ciufo DM, Alcendor DJ, Cannon JS, Ambinder R, Orenstein JM, Reitz MS, Hayward GS.** 1999. Comparison of genetic variability at multiple loci across the genomes of the major subtypes of Kaposi's sarcoma-associated herpesvirus reveals evidence for recombination and for two distinct types of open reading frame K15 alleles at the right-hand end. J. Virol. **73:**6646–6660.
100. **Lagunoff M, Ganem D.** 1997. The structure and coding organization of the genomic termini of Kaposi's sarcoma-associated herpesvirus. Virology **236:**147–154.
101. **Wong EL, Damania B.** 2006. Transcriptional regulation of the Kaposi's sarcoma-associated herpesvirus K15 gene. J. Virol. **80:**1385–1392.
102. **Russo JJ, Bohenzky RA, Chien MC, Chen J, Yan M, Maddalena D, Parry JP, Peruzzi D, Edelman IS, Chang Y, Moore PS.** 1996. Nucleotide sequence of the Kaposi sarcoma-associated herpesvirus (HHV8). Proc. Natl. Acad. Sci. U. S. A. **93:**14862–14867.